Journal of Applied Mechanics and Technical Physics, Vol. 45, No. 4, pp. 486–497, 2004

EXPERIMENTAL INVESTIGATION OF THERMOCAPILLARY CONVECTION INDUCED BY A LOCAL TEMPERATURE INHOMOGENEITY NEAR THE LIQUID SURFACE. 1. SOLID SOURCE OF HEAT

A. I. Mizev

UDC 532.6;532.5:532.5.013.4

The structure and stability of a thermocapillary flow from a concentrated source of heat located near the free surface of the liquid filling a deep reservoir are experimentally studied. For a certain power of the heat source, oscillatory instability leading to formation of surface waves is observed. Possible mechanisms of the observed instability are discussed.

Key words: *thermocapillary convection, source of heat, flow instability, surface waves.*

Introduction. The study of capillary flows generated by an inhomogeneity in temperature conditions along the interface between the phases is of interest not only from a purely academic viewpoint but also for particular practical applications. Such flows should be taken into account in solving numerous scientific and engineering problems, such as, e.g., separation of admixtures, obtaining relief photographic images, surface alloying of metals, curing of some pulmonary diseases, etc. The special interest in thermocapillary flows, associated with the nongravitational nature of this mechanism of convection, is inspired by the development of new technologies in the field of space material science.

Many theoretical and experimental works on this topic have been published recently (see, e.g., [1–3]). A review of experimental works shows, however, that the stability of a capillary flow is normally considered in rather thin layers of the liquid. This, in the authors' opinion, allows one to neglect the contribution of the free-convection mechanism of convection, as compared to the thermocapillary mechanism. Such a choice of problem geometry incurs a specific evolution of the system: already at comparatively low velocities, the flow becomes unstable to vortical disturbances developed at the boundary of the surface and bottom flows existing in a rather narrow region of the liquid. Instability in the form of standing or running (depending on the Prandtl number of the working liquid) vortices arising at the boundary of opposing flows was found in [4–6]. As it will be shown in the present work, the intensity of thermocapillary and thermogravitational convection is commensurable in the case of a deep reservoir as well. The competition of both types of convection produces new effects that were not observed previously.

Theoretical investigations of thermocapillary convection from concentrated sources of heat located on a free nondeformable surface of the liquid (see, e.g., [7–9]) also limit the class of phenomena considered, artificially imposing flow evolution related to instability in the liquid volume only. As was shown in [10–12], however, an integral attribute of thermocapillary flows is the curvature of the free surface, which, in turn, can affect the structure of the arising flow and lead to its instability.

In the present work, we describe the results of experimental investigations of stability of a thermocapillary flow from a concentrated source of heat located near the free surface of the liquid filling a deep (as compared to the heat-source size) reservoir. It is shown that thermocapillary effects can also lead to significant changes in the flow structure and heat-transfer intensification in rather deep reservoirs with developed free convection. The results

Perm' State University, Perm' 614990. Translated from Prikladnaya Mekhanika i Tekhnicheskaya Fizika, Vol. 45, No. 4, pp. 36–49, July–August, 2004. Original article submitted August 11, 2003; revision submitted December 8, 2003.

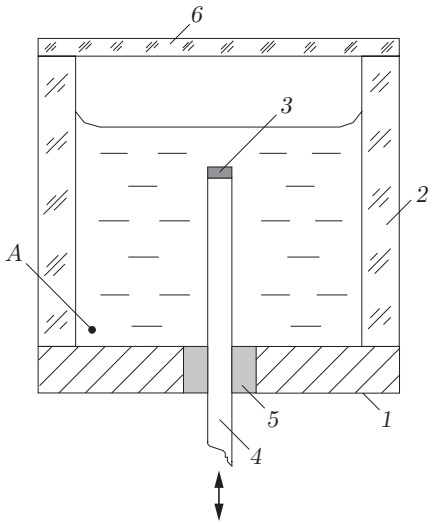

Fig. 1

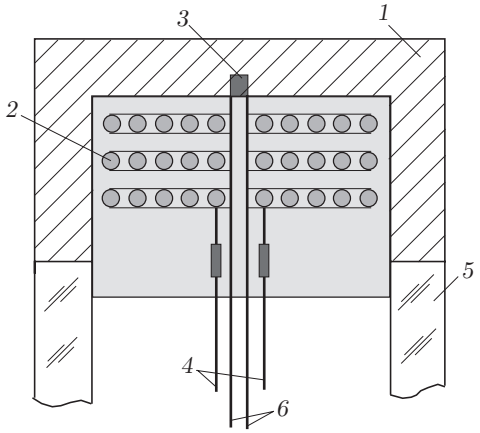

Fig. 2

Fig. 1. Layout of the convective chamber.

Fig. 2. Layout of the heating element of the source of heat.

are compared with other experimental works to clarify the instability mechanisms leading to origination of surface waves observed in the present work.

Experimental Setup and Measurement Techniques. Experimental investigations of instability of thermocapillary flows is a separate, rather complicated class of researches in mechanics of continuous media. This is primarily caused by the close relation between convective flows and interface parameters. Flows arising in the liquid volume can lead to changes in temperature conditions on the surface or to deformations of the latter. There is always some feedback, however, when the change in conditions on the liquid surface exerts a significant effect on characteristics and stability of the flow itself. The reasons for instability in the problem can be hydrodynamic, thermal, or surface processes. A successful study of instability of thermocapillary flows is intimately related to the necessity of simultaneous measurements of the structure of convective motion itself and of the liquid-surface shape. For this purpose, we developed an experimental setup that allows simultaneous thermal and optical measurements.

The main element of this setup is a convective chamber (Fig. 1) with a base of 100×100 mm and 110 mm high. A transparent glass frame 2 limiting the size of the cavity was glued onto the base 1 made of fabric-base laminate. A source of heat 3 shown schematically in Fig. 2 was placed into the cavity. The shell 1 of the heating element was a brass cylindrical glass 2 mm high. The outer diameter was chosen such that the source of heat could be approximated as a point source. Heaters with outer diameters of 5 and 7 mm were used in the experiments. The shell thickness was 0.7 mm everywhere. A small-diameter blind hole was drilled at the center of the "bottom", and the junction 3 of the differential copper–Constantan thermocouple was welded into this hole. The second junction was located in a liquid region remote from the heater (point A in Fig. 1). The shell of the heating element contained a thin (0.1 mm in diameter) manganin wire 2 electrically insulated from the external shell. At the heater output, the ends of the manganin wire were welded to input copper wires 4 from the power source. The heating element 4 (see Fig. 1) was glued to a glass tube 5, which had the same diameter as the shell. The tube contained input wires 4 (see Fig. 2) from the power source and wires 6 from the thermocouple. The opposite end of the tube was driven outside the cavity through a hole in the base and attached to a micrometric site used to move the heater in the vertical direction. The depth of the heat source relative to the liquid surface could be changed within 0.1 mm. To prevent liquid outflow from the convective cavity, the hole in the base was sealed by a fluoroplastic gasket 5 (Fig. 1). The change in the height of the liquid layer above the heat source because of liquid outflow was less than 0.01% during one experiment. On the top, the convective cavity was closed by a transparent glass plate. The presence of the plate reduced the intensity of evaporation from the liquid surface and prevented origination of random air streams capable of producing a nonequilibrium distribution of surface tension because of nonuniform evaporation along the

liquid surface. Preliminary experiments showed that the presence or absence of the plate bounding the vapor–gas space has no effect on the flow structure and quantitative results of thermal measurements, which indicates that the intensity of evaporation from the free surface of the liquid is very low. Hence, during filming of surface waves, the plate was removed to obtain a better quality of the image.

The liquid under study was *n*-decane ($C_{10}H_{22}$). The choice of the working liquid was caused by a rather low coefficient of surface tension of decane (23.9 mN/m at 20°C), which prevents the formation of an adsorbed film of the surface-active material on the surface. The presence of such a film can lead to stabilization of surface flows and sometimes even prevent their origination. At the same time, this liquid has a rather high temperature coefficient of surface tension [0.092 mN/(m · K)], which allows obtaining high-intensity thermocapillary flows. The liquid temperature before the experiment was set in the range of 20–23°C.

The quantities measured during the experiment were the heater power, the depth of its immersion, and the temperature of the heater shell relative to the undisturbed (point A in Fig. 1) region of the liquid. Addition of a small amount of light-scattering particles into the liquid under study and the use of the "laser sheet" allowed simultaneous visualization of the structure and measurements of quantitative characteristics of emerging flows.

For a quantitative study of the liquid-surface shape, a specially developed method of a "scanning slot" was used. The essence of the method is the analysis of a specifically shaped light front reflected from the interface. The light from the light source (in our case, a laser) is transformed to a plane–parallel beam by the optical system. Then, a diaphragm cuts a light beam from the wave front incident onto the liquid surface; the beam has the form of a narrow slot. The shape of the reflected image of the slot is observed on a screen. If the liquid surface is flat, the image coincides with the shape of the diaphragm used to form the image. If the liquid surface is curved, however, the image of the slot on the screen is distorted, and it is possible to reconstruct the profile of the part of the liquid surface responsible for reflection on the basis of deviations from the initial shape. Moving the diaphragm in the direction transverse to the slot, we obtain the profile of the neighboring cross section of the surface, etc. Scanning the entire width of the cavity in this manner, we can reconstruct the shape of the entire surface of the liquid. The sensitivity of the method can be changed by changing the distance between the surface and the screen. The maximum possible distances are chosen so that diffraction distortions do not interfere with slot-image reconstruction. The maximum reachable sensitivity of the method under these restrictions is approximately 0.1 μm.

Investigation of Heat-Release Regimes. The experiments were performed with an open or covered surface of the liquid. In the second case, the liquid surface was covered by a glass plate, which allowed us to completely eliminate capillary effects. The experiments showed that, as the source of heat approaches the free surface of the liquid, the temperature of the heat-source surface relative to the deep layers of the liquid considerably decreases, which indicates an increase in heat release from the heater. In the opposite case (covered surface), the heat release decreases.

Figure 3 shows the typical dependences of the heater-surface temperature on the depth of heater immersion for two values of the source power. For rather high values of immersion depth, the heat-release regimes are identical for the cases of the open and covered surfaces of the liquid. In both cases, visual observations reveal the presence of a flow in the form of a thermal plume with a rather low characteristic value of velocity. Beginning from distances to the surface commensurable with the heater diameter, the character of heat release into the liquid becomes significantly different. As the source of heat approaches the free surface of the liquid, the heat release from the source noticeably increases. The reason is the origination of thermocapillary flows on the free surface of the liquid. This is also evidenced by visual observations. As the source of heat approaches the free surface of the liquid, the region of existence of convective flows is shifted to the subsurface layer and forms a toroidal convective cell typical of a thermocapillary flow with a given geometry of the problem [4, 6, 12]. The characteristic value of velocity, which is maximum on the liquid surface, considerably increases, reaching several centimeters per second. A further decrease in the distance between the source of heat and the free surface of the liquid leads to an insignificant increase in temperature of the heat-source surface in the range of low depths because of the appearance of a region of contact between the heat source and the gas phase. As is seen from the figure, the contact with the liquid surface occurs at a nonzero value of immersion depth. The reason is the curvature of the liquid-surface shape above the heat source toward the liquid phase. In this case, the heat release decreases in proportion to the area of contact between the heater shell and the gas phase whose thermal conductivity is much lower than the thermal conductivity of the liquid phase.

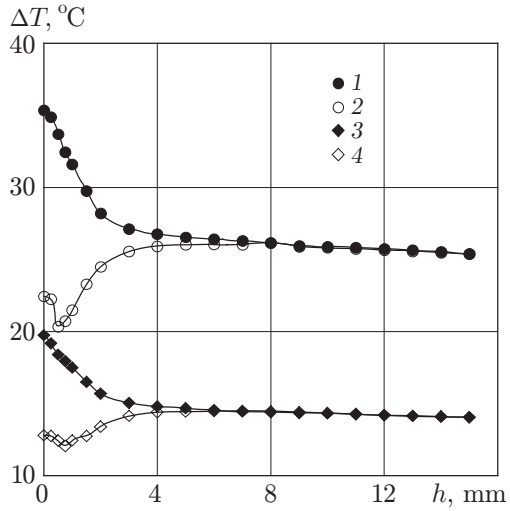

Fig. 3. Temperature of the heating element versus the depth of immersion of the heat source (the heat-source diameter is $d = 7$ mm): curves 1 and 2 refer to covered and free surfaces for $P = 1.25$ W, respectively, curves 3 and 4 refer to covered and free surfaces for $P = 0.6$ W, respectively.

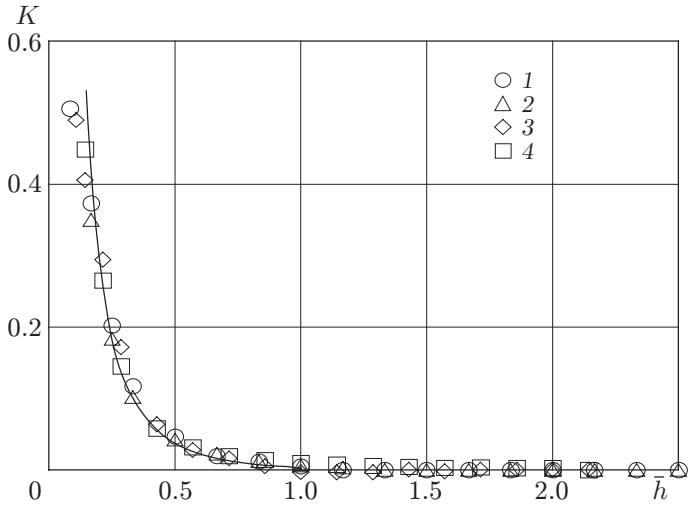

Fig. 4. Parameter K as a function of the dimensionless immersion depth of the heat source: $d = 5$ mm and $P = 0.7$ W (1); $d = 5$ mm and $P = 1.32$ W (2); $d = 7$ mm and $P = 0.6$ W (3); $d = 7$ mm and $P = 1.25$ W (4).

Based on the measurement results, we constructed the intensity of thermocapillary motion as a function of the dimensionless depth of immersion of the heat source for different values of heater power (Fig. 4). The immersion depth is normalized to the diameter of the heating element. As a measure of intensity of thermocapillary flows, we chose the dimensionless ratio $K = T_c/T_f - 1$, where T_c and T_f are the temperatures of the heating element in the case of the covered and free surfaces of the liquid, respectively. This quantity is an analog of the Nusselt number for this problem and has the meaning of the ratio of heat release due to capillary effects to the sum of heat losses caused by molecular transfer and free-convective motion minus unity. The influence of thermocapillary effects is manifested at distances to the surface smaller than or comparable to the heat-source diameter. The heat release due to thermocapillary convection is higher than the heat release due to thermogravitational convection by more than a factor of 1.5.

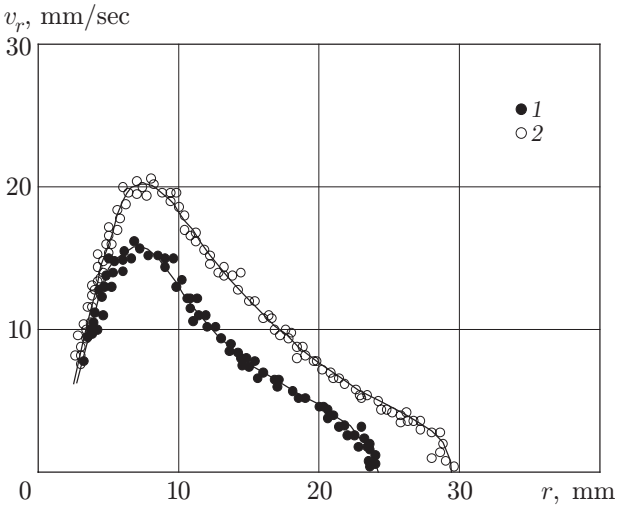

Fig. 5. Radial component of flow velocity on the liquid surface versus the radial coordinate: the origin coincides with the center of the heat source; the power of the heating element is $P = 0.61$ W; the immersion depth is $h_0 = 10$ (1) and 1 mm (2).

Effect of Power and Immersion Depth of the Heat Source on the Flow Structure. Observations of the flow structure showed that the flow is localized in space and is a toroidal convective cell symmetric with respect to the vertical axis passing through the source of heat. The cell is characterized by a clearly expressed size. The liquid outside the convective cell is motionless, which is evidenced by the absence of tracks in these regions of the liquid. The study of the flow structure showed that the character of liquid motion remains qualitatively unchanged. For all powers that could be reached in the experiments and immersion depths of the heat source, the flow remains radially symmetric. An increase in power or a decrease in the distance between the source of heat and the interface only increases the cell diameter.

In addition to changes in the size of the convective cell itself, the changes in power and immersion depth of the heat source alter the characteristic flow velocity. Figure 5 shows the radial component of velocity on the surface as a function of the distance to the heater. For comparison, the velocity profiles for two different positions of the heat source relative to the liquid surface for an identical power are shown. The velocity distribution has a maximum whose position depends on the immersion depth of the heater. As the heat source approaches the surface, the velocity maximum is shifted to the periphery. Nevertheless, despite the changes in velocity characteristics of the flow, the character of the dependence of velocity on the radial coordinate remains unchanged.

When the immersion depth of the heat source is changed, the size of the region of existence of convective motion changes not only in the radial direction. When the heater approaches the liquid surface, the flow acquires a subsurface character. This is also evidenced by the quantitative studies of the velocity distribution in the liquid. Figure 6 shows the radial component of flow velocity in the liquid volume versus the distance to the surface for different immersion depths. As the source approaches the surface, the velocity of liquid motion in the cell increases. The depth of penetration of the flow inward the liquid decreases. The entire centrifugal flow is concentrated in a rather narrow ($h \approx 2{-}3$ mm) subsurface region.

Effect of the Convective Flow on the Liquid-Surface Shape. For all values of problem parameters, power, and immersion depth of the heat source, the boundary of the liquid near the source is always deformed. The liquid surface becomes curved and acquires this or that shape, depending on the character and intensity of flows arising in the liquid. Visual observations revealed two basic modes of instability of the liquid surface: steady and oscillatory ones.

Figure 7 illustrates the shape of the liquid surface for different immersion depths with a fixed power of the heater. The surface is cut by the vertical plane passing through the center of the heat source whose position is shown in the figure. The dashed curve indicates the position of the undisturbed boundary.

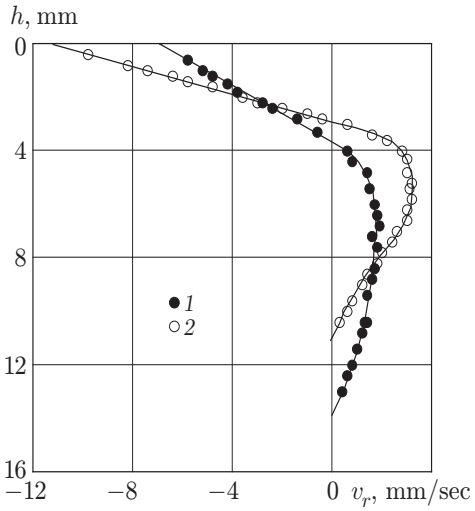

Fig. 6. Radial component of flow velocity in the liquid volume versus the distance to the surface ($P = 0.61$ W): curves 1 and 2 refer to the immersion depth of the heat source $h = 10$ and 1 mm, respectively.

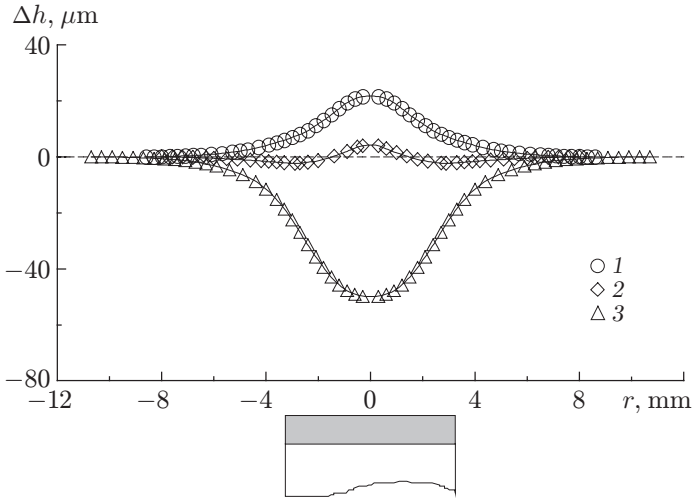

Fig. 7. Surface shape versus the coordinate along the surface for different positions of the heat source for $P = 0.8$ W and $h = 9$ (1), 2.3 (2), and 1.2 mm (3).

For rather large immersion depths of the heat source, when the thermocapillary flow intensity is yet rather low, the governing role belongs to flows caused by the thermogravitational mechanism of convection excitation. A typical feature of such a flow for the case considered is the presence of a thermal plume propagating from the heat source to the liquid surface and responsible for surface curvature toward the gas phase (curve 1 in Fig. 7). As the heat source gradually approaches the liquid surface, the contribution of the thermocapillary mechanism of convection to the overall pattern of the flow starts to increase. The intensity of axisymmetric radial motion along the surface also increases and leads to a smaller curvature of the liquid surface. With a further decrease in the immersion depth of the heat source, when the thermocapillary flow intensity becomes commensurable with the thermogravitational flow intensity, the convex shape is supplemented by a surface region with the opposite curvature (curve 2 in Fig. 7). Subsequent approaching of the heat source to the surface changes the sign of curvature of the liquid surface, i.e., the surface becomes curved toward the liquid phase and acquires a funnel shape (curve 3 in Fig. 7). For all positions of the heat source, the surface profile is symmetric with respect to the vertical axis passing through the center of the heating element. The figure formed by revolution about this axis yields a three-dimensional pattern of the liquid-surface shape.

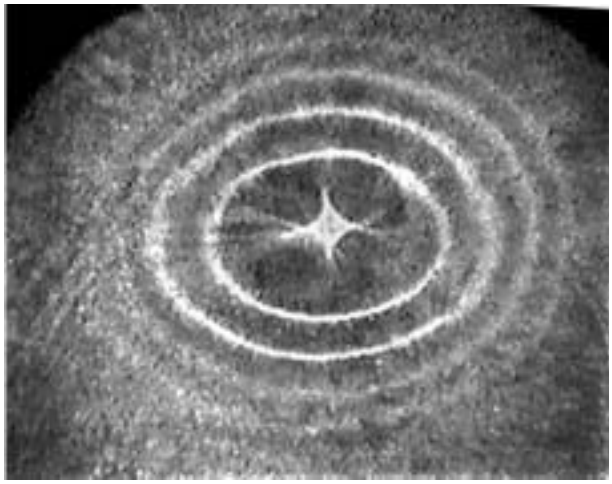

Fig. 8. Photograph of the circular wave on the liquid surface for $P = 1.5$ W and $h_0 = 1.1$ mm.

For a certain threshold value of the immersion depth of the heater, depending on the heater power, the surface shape is no longer stationary and acquires an oscillatory character. The curvature of the liquid surface above the heater fluctuates periodically about a certain equilibrium value, which leads to formation of surface waves propagating from the heat source. The configurations of the arising waves depend on the distance to the surface and on the heater power.

Investigation of Surface Waves. The above-described method of the "scanning slot" is fairly well applicable to measurements of the stationary shape of the surface. If waves arise on the liquid surface, however, the information value of this method rapidly decreases, since the method makes it possible to obtain information about a certain cross section of the wave and does not allow reconstruction of the complete pattern at a particular time. Therefore, another method is used in such situations; the optical scheme in this method differs by the absence of the diaphragm only. The entire surface area in this case is illuminated by a wide plane–parallel light beam. Light is reflected from the concave part of the wave as if from a collecting mirror, which increases the intensity at the corresponding point on the screen. Vice versa, the intensity of light reflected from the convex part of the wave and incident onto the screen is lower. The shape of the light-intensity distribution on the screen will repeat the shape of the wave on the liquid surface. It is only necessary to choose the distance to the screen corresponding to the greatest possible contrast of the image. This method cannot be used for quantitative measurements of the surface profile and is applied only for visualization of surface waves.

If the heat-source immersion depth is comparatively large, surface oscillations induce surface waves, which are concentric circles (Fig. 8). As the heater approaches closer, this shape of the wave becomes unstable, and a new configuration is formed, which is a spiral wave rotating to the right or to the left (Fig. 9). The direction of rotation at the moment of formation of this wave has a random character, i.e., the probabilities of formation of a wave with right or left swirl are identical. A decrease in immersion depth of the heater leads to an increase in the azimuthal wavenumber, which is manifested as an increase in the number of branches of the spiral wave. Figure 9 shows the evolution of the spiral-wave configuration for the heat source approaching the free surface of the liquid. Spiral waves with the number of branches from one to ten were obtained in the experiments. Further approaching of the heat source is responsible for the contact between the heating element and the liquid surface concave toward the liquid phase. Liquid-surface oscillations are terminated, and a stationary standing wave structure with a beam configuration is formed on the surface (Fig. 10).

As was noted above, the critical value of immersion depth at which the shape of the liquid surface becomes unstable to oscillatory disturbances depends on the heat-source power. Figure 11 shows the chart of surface-shape stability in coordinates power–immersion depth. As the power of the heat source increases, the experimentally observed wave instability occurs at greater values of immersion depth. The change in the spiral configuration of the waves is not indicated inside the region of existence of spiral waves. The reason is that the range of immersion

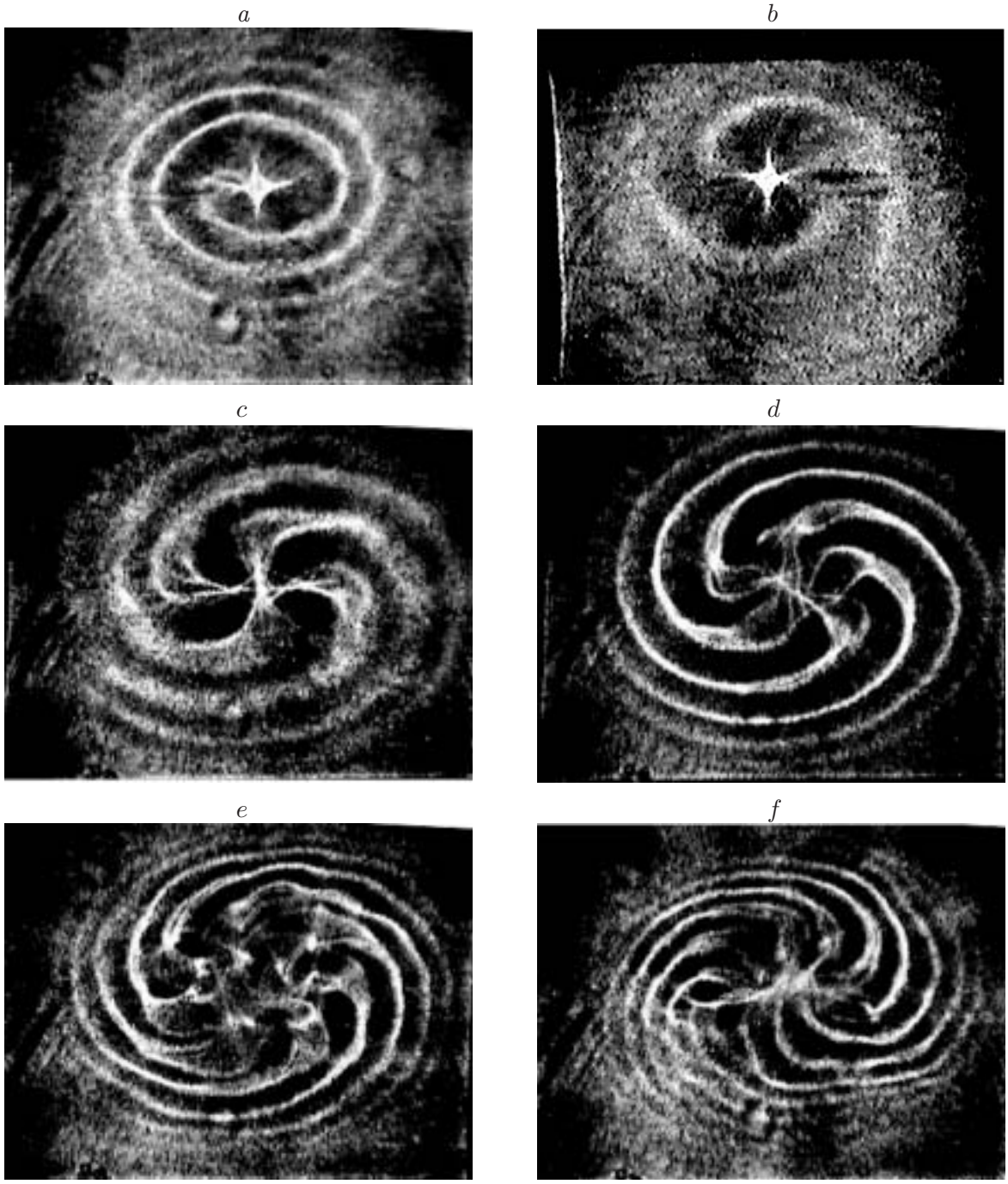

Fig. 9. Evolution of a spiral wave (a–f) as the heat source approaches the liquid surface for $P =$ 1.5 W; the immersion depth changes from 0.9 to 0.6 mm.

depths at which the spiral configuration of the wave is observed is very narrow (no more than 0.4 mm for the maximum reachable powers). The accuracy with which the immersion depth can be measured is 0.1 mm. Thus, the width of the existence region of spiral waves with a certain fixed topological charge is smaller than the least immersion depth that can be measured in the setup. This is especially well manifested for waves with a large number of branches, because the width of the existence region of waves with this or that value of the topological charge decreases as the latter increases.

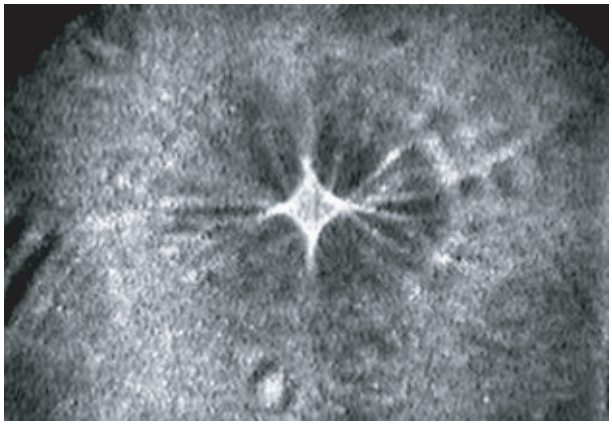

Fig. 10. Photograph of the standing wave structure with a beam configuration on the liquid surface for $P = 1.5$ W and $h_0 = 0.5$ mm.

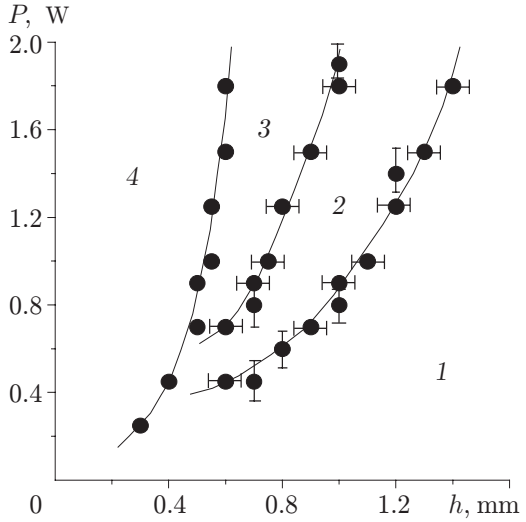

Fig. 11. Chart of stability of the surface shape in coordinates of power and immersion depth. The numerals on the figure indicate the regions of existence of the stationary shape of the surface (1), circular configuration of the wave (2), spiral configuration of the wave (3), and contact between the source and the liquid surface (4).

To study the characteristics of waves formed on the liquid surface, we constructed a space–time diagram of wave motion. Let us choose a certain radial direction corresponding to a fixed value of the azimuthal angle and mark the change in the radial coordinate of individual parts of the wave front in time. The vertical and horizontal cross sections of such a dependence yield information on the spatial and temporal frequency of oscillations, and the derivative of this dependence yields the wave velocity at an arbitrary point. Figure 12 shows the dependences for waves of different configurations: circular wave (a) and two spiral waves (b and c) with different numbers of branches. The space–time characteristics of these two types of waves are significantly different. An analysis of Fig. 12a shows that typical features of circular waves are a constant radial velocity of wave-front propagation and a constant radial wavenumber. The situation becomes different if the circular wave is changed by the spiral wave. As it follows from Fig. 12b, the space–time dependence becomes nonlinear, which indicates that wave propagation from the source is nonuniform. The radial component of the wave-front velocity decreases as the wave propagates toward the periphery. Therewith, the radial wavenumber increases. These effects are manifested more clearly as the number of spiral branches increases (Fig. 12c). The waves considered, however, have also a common feature. With a sufficient distance from the center, the space–time characteristics become identical: the velocity and spatial

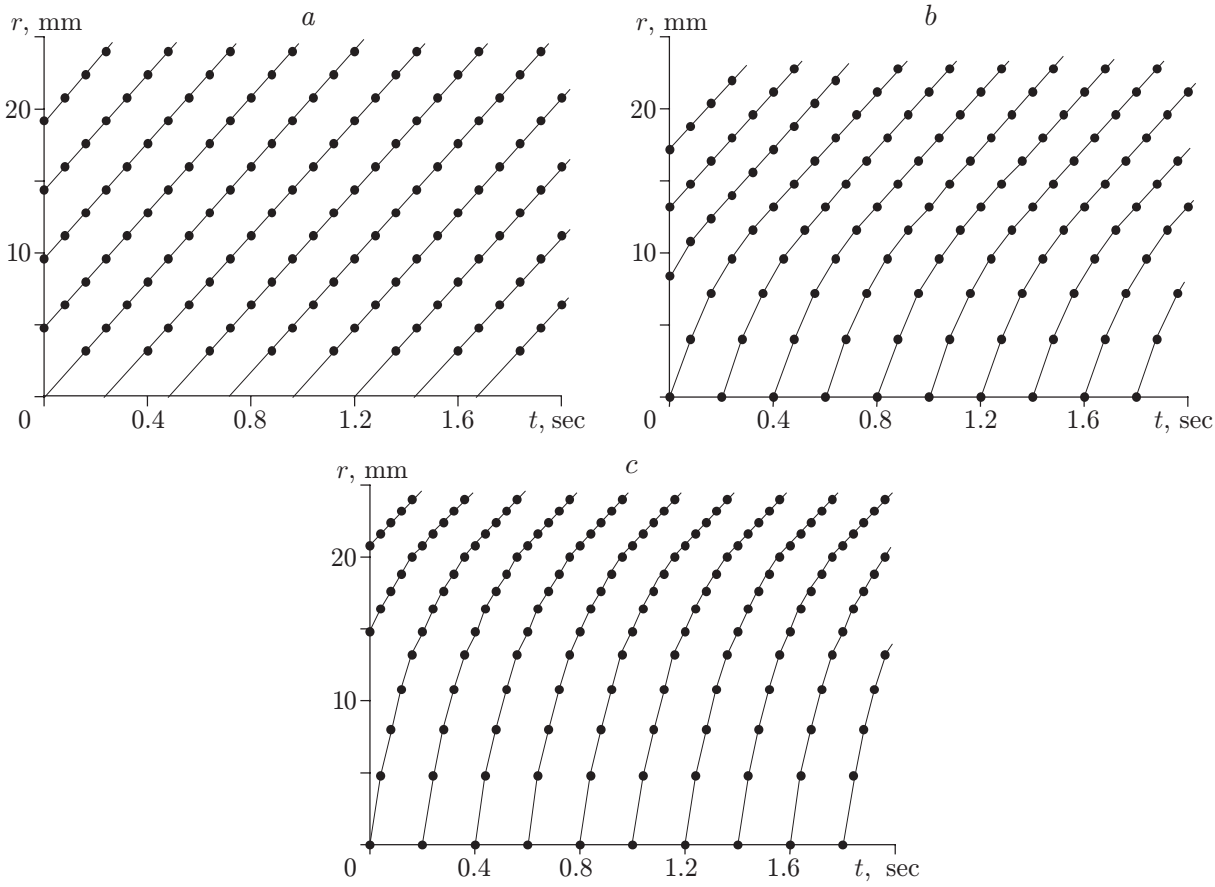

Fig. 12. Space–time diagram of wave motion: circular wave (a), spiral wave with three branches (b), and spiral wave with five branches (c).

frequency of spiral waves tend to values typical for a circular wave. Figure 13 shows the radial velocity for waves of different configurations versus the distance to the heat source. For comparison, the dashed curve shows the same dependence for the flow velocity on the surface. One can see that there are regions where the wave moves faster than the flow or lags behind the latter.

We try to explain the dependence on the spatial frequency of spiral waves on the distance to the heat source. This is even more interesting because this feature has not been observed in similar wave structures until now [13–15]. It does not seem possible to explain such a behavior of the wave front by the dependence of the surface-tension coefficient on temperature because, in this case, a strictly opposite pattern of the decrease in the radial wavenumber would be observed. One possible real explanation is as follows. It is seen from the analysis of the images of spiral waves in Fig. 9 that the propagating wave is a superposition of a set of waves. This is especially noticeable for waves with a large number of spirals: the wave front in the beginning of its propagation is "modulated" by the short-wave component. The dispersion characteristics of the waves that form such a "packet" are usually different. Shorter waves usually have a higher decay coefficient. It seems that, in the case considered, the decay of individual parts of the wave "packet" alters the characteristics of the latter. The identity of characteristics of the spiral and circular waves at the periphery becomes understandable.

In the course of the present research, we tried to find the reasons for vibrational instability of the liquid surface. As was already noted, the specific feature of the flow under consideration is a close relationship between the convective flow and interface. Therefore, the surface curvature can be related to the change in the flow structure in the liquid. As it follows from the results described above, the maximum distortions of the surface and origination of surface waves occur in a moderate region directly above the heat source. Comparing the linear size of this region of the liquid (the source diameter is 5–7 mm) with its transverse size (the waves appear at a depth $h \approx 0.7{-}1.2$ mm),

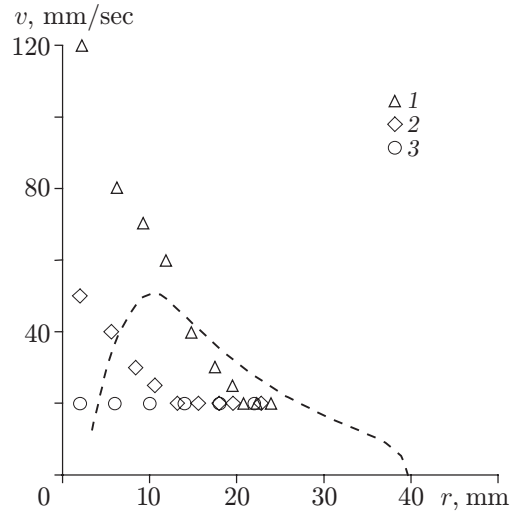

Fig. 13. Radial velocity of waves of different configurations versus the distance to the heat source: spiral waves with three (1) and five (2) branches, circular wave (3), and the dashed curve shows the radial flow velocity.

we can rather accurately represent it as a flat horizontal layer with a free upper boundary along which the radial temperature gradient is specified. An analysis of available publications showed that there are some experimental investigations of this problem geometry. Favre et al. [4] considered flow instability in a flat horizontal layer with a free upper boundary containing a concentrated source of heat on the surface. In this case, an axially symmetric flow is generated; the flow is directed away from the center on the surface and toward the center of the cavity at the bottom; for a certain ratio of the layer height, its diameter, and heater power, the flow becomes unstable. Various secondary flows arise successively in the volume of the liquid. The first type of flow consists of concentric waves propagating toward the heat source. The second type of secondary flows has the form of beam-shaped waves rotating relative to the axis passing through the cavity center. The number of "beams" depends on the problem parameters. It seems probable that such a type of flow instability in the case considered in the present paper can occur in the region directly above the heat source. When the first type of the secondary flow is formed, the waves "converging" toward the center periodically distort the surface shape, inducing circular waves. Rotating beam-shaped waves can give rise to branches of the spiral wave. Because of the small size of the region of the liquid above the heat source, a direct study of the secondary flow for verification of the assumption made above is an extremely complicated problem.

This work was supported by the Russian Foundation for Basic Research (Grant Nos. RFBR-Ural 02-01-96407 and 04-01-96029).

REFERENCES

1. J. Pantaloni, B. Bailleux, J. Salan, and M. J. Velarde, "Rayleigh–Benard–Marangoni instability: New experimental results," *J. Non-Equil. Thermodyn.*, **4**, 201–218 (1979).
2. V. V. Pukhnachov, "Thermocapillary convection under low gravity," *Fluid Dyn. Trans.*, **14**, 145–204 (1989).
3. V. G. Levich and V. S. Krylov, "Surface-tension driven phenomena," *Ann. Rev. Fluid Mech.*, **1**, 293–316 (1969).
4. E. Favre, L. Blumenfeld, and F. Daviaud, "Instabilities of a liquid layer locally heated on its free surface," *Phys. Fluids*, **9**, No. 5, 1473–1475 (1997).
5. A. B. Esersky, A. Garcimartin, H. L. Mancini, and C. Perez-Garcia, "Spatiotemporal structure of hydrothermal waves in Marangoni convection," *Phys. Rev. E*, **48**, No. 6, 4414–4422 (1993).
6. A. B. Esersky, A. Garcimartin, J. Burguete, et al., "Hydrothermal waves in Marangoni convection in a cylindrical container," *Phys. Rev. E*, **47**, 1126–1131 (1993).

7. Y. Kamatani, A. Chang, and S. Ostrach, "Effects of heating mode on steady axisymmetric thermocapillary flows in microgravity," *J. Heat Transfer*, **118**, 191–197 (1996).
8. Yu. K. Bratukhin and S. O. Makarov, "Secondary thermocapillary motion of the soliton type," *Izv. Ross. Akad. Nauk, Mekh. Zhidk. Gaza*, No. 4, 20–27 (1992).
9. V. Shtern and F. Hussain, "Azimuthal instability of divergent flows," *J. Fluid Mech.*, **256**, 535–560 (1993).
10. A. F. Pshenichnikov and G. A. Tokmenina, "Deformation of the free surface of the liquid by thermocapillary motion," *Izv. Akad. Nauk SSSR, Mekh. Zhidk. Gaza*, No. 3, 150–153 (1983).
11. V. V. Nizovtsev, "Investigation of natural convection and convection stimulated by local irradiation in a thin layer of evaporating liquid," *J. Appl. Mech. Tech. Phys.*, **30**, No. 1, 132–138 (1989).
12. V. V. Nizovtsev, "Capillary convection in a liquid layer under laser radiation," *Inzh.-Fiz. Zh.*, **55**, No. 1, 85–92 (1988).
13. A. M. Zhabotinskii, *Concentration Oscillations* [in Russian], Nauka, Moscow (1974).
14. M. V. Nezlin and E. N. Snezhkin, *Rossby Vortices and Spiral Structures: Astrophysics and Plasma Physics in Shallow-Water Experiments* [in Russian], Nauka, Moscow (1990).
15. M. I. Rabinovich and D. I. Trubetskov, *Introduction into the Theory of Oscillations and Waves* [in Russian], Nauka, Moscow (1992).